Experimental study on partial oxy-combustion technology in a bench-scale CO_2 capture unit

F. Vega, S. Camino, L. M. Gallego, M. Cano, B. Navarrete

Chemical and Environmental Engineering Department, School of Engineering, University of Seville, C/ Camino de los Descubrimientos s/n 41092 Sevilla, Spain, Phone: 954481397, fvega1@etsi.us.es

Abstract

The reduction of CO_2 emissions from anthropogenic sources in this century will require a higher reliance on carbon capture and storage (CCS) technologies. Post-combustion based on a regenerative chemical absorption is considered a mature and close-to-market option in near and mid-term. However, the high energy penalty related to solvent regeneration and solvent degradation are two of the main drawbacks hindering the deployment of this technology. Partial oxy-combustion is considered a promising CCS technology that can substantially decrease the reboiler duty due to the increase on the CO_2 partial pressure in the flue gas and hence the driving force in the absorber compared to conventional post-combustion approaches. This work explores the potentialities of partial oxy-combustion in a bench-scale CO_2 capture unit to evaluate the benefits on the CO_2 separation stage. The experimental facility consists of a regenerative CO_2 chemical absorption process with a CO_2 removal capacity of 0.48 kg/h. The most relevant operating parameters such as temperature, CO_2 loading and L/G ratios were evaluated under variations of the CO_2 concentration of the flue gas, ranging between 15%v/v and 60%v/v CO_2, in order to obtain the optimal reboiler duty associated to the solvent regeneration. Results showed that the use of four packing bed improved the CO_2 absorption performance. Although the optimal L/G ratios were moved to higher values, they also achieved CO_2 removal efficiencies over 95% and lower energy consumptions compared with the baseline case (post-combustion). Experiments carried out using a 60%v/v CO_2 in the flue gas provided 95.7% of CO_2 removal efficiency and the lowest reboiler duty (4.74 GJ/t CO_2) which resulted in a 57% reduction of the specific energy consumption compared with the post-combustion run.

Keywords: absorption, bench-scale, CCS, CO_2 capture, partial oxy-combustion

1. Introduction

Global energy demand has experienced a substantial increase over last decades. Despite the efforts made in renewable energy development in recent years and the growth of non-fossil energy, such us nuclear and hydropower, the contribution of fossil-fuels in primary energy production might be considered almost unchanged over the last 40 years - from 86.7% in 1973 to 81.7% in 2012 and 81.4% in 2013 - and continues to be the main source for supplying the energy demand [1]. The use of fossil fuels as an energy source is considered the largest anthropogenic CO_2 emission contributor worldwide and coal-fired power plants are responsible of more than 70% of the CO_2 emissions related to the energy production sector [2, 3].

The global energy landscape described above requires an international awareness and global cooperation in order to restrict the worse consequences of global warming. The Conference of Parties (COP-21), held at the end of 2015 in Paris, concluded with the Paris Agreement which is considered an historic step forward to combat climate change, unleash actions and investment towards a low carbon, resilient and sustainable future. The COP-21 agreement's aim is to keep a global temperature rise this century well below 2˚C and to drive efforts to limit the temperature increase even further to 1.5˚C above pre-industrial levels [4]. This target will require greater reductions in CO_2 emissions from 2030 to 2050, speeding up the scale-up of low-carbon energy technologies over this period, and also higher reliance on carbon capture and storage (CCS) technologies. In fact, CCS is considered a front line approach that should play a relevant role towards low-carbon energy production. Their contribution is estimated around 13-15% of the overall CO_2 emission reduction target aimed by 2030 [5, 6].

Among the main alternatives of CCS, post-combustion CO_2 capture based on amine scrubbing is the most promising and close-to-market CCS approach. However, there are several drawbacks that constrain the deployment of post-combustion technology and its use in fossil-fuels power plants. In particular, the main drawbacks are listed as follows: (a) high capital cost and large

equipment size, (b) high energy penalty related to solvent regeneration, (c) solvent loss derived from degradation process, (d) volatile solvent emission that can potentially produce nitramines and nitrosamine compounds and (e) corrosion issues [7-10]. The high energy penalty required for CO_2 stripping is the largest barrier hindered the deployment of CO_2 chemical absorption for carbon capture at industrial scale. In fossil-fuel power plants, this energy demand is supplied using steam extractions from the power cycle that should reduce the net power efficiency in 7-14% points [11, 12].

In last decades, efforts are driven towards novel solvent/blend development. Novel tertiary amines such as N,N-diethylethanolamine (DEEA) has been proposed in order to provide a hybrid behaviour of amine-based blends [13]. Recent studies of biphasic solvent blends has shown up to 50% reduction of the heat duty compared to the MEA 30wt% benchmark [14]. It should be noted ionic liquids have become a promising alternative as solvents for CO_2 capture applications [15]. New process configurations [16] and heat integration of the conventional CO_2 absorption-desorption layout [17, 18] led to further reductions of the regeneration energy penalty and hence the enhancement of the thermal energy efficiency of the overall energy production combined with CCS process.

A large summary of the CCS pilot plant installations have been utilized for developing chemical absorption applied to CCS in recent years. The capture capacity of the pilot plants range between two levels. Installations with low CO_2 capacity are able to capture from 0.1-1 t CO_2/day, whereas higher capacities are in the range between 10-80 t CO_2/day [19-21]. The reboiler duty associated with MEA typically is reported as 3.5-4.2 GJ/t [21 – 23]. The regeneration energy of most of the solvents can be found in the range of 3-4 GJ/t CO_2 [24, 25], but only two references report values below 3 GJ/t CO_2. DOW in collaboration with ALSTOM developed the undisclosed proprietary solvent named URCASOL™, which can reduce the energy requirement for CO_2 desorption up to 2.3 GJ/t CO_2 [26]. However, these institutions are primarily focused on developing the chilled ammonia process [27]. IHI also obtained low reboiler duties, ranging between 2.5-2.6 GJ/t CO_2,

during its test campaigns at the Aioi pilot plant using different amine blends, namely ISOL´s [28]. An experimental test programme at a 100 t CO_2/day CCPilot100+ capture plant at the Ferrybridge Power Station was concluded in December of 2013 using MEA 30wt% and RS-2™ solvents. This novel solvent exhibited a high performance and its energy regeneration was significantly lower than MEA cases [29]. Rabensteiner et. al. carried out a test campaign at a test facility at CO_2 SEPPL pilot plant located at the power plant in Dürnrohr (Austria) using a novel blend consisted of an aqueous solution of 28wt% 2-amino-2-methyl-propanol (AMP) and 17wt% piperazine (PIP). The minimal specific energy for solvent regeneration was 3.15 GJ/t CO_2, resulting in a 10% energy reduction compared with MEA 30wt% tests. The CO_2 concentration in the flue gas varied from 11.6%v/v to 13%v/v. Other studies performed at pilot plant scale evaluated the solvent degradation [31]. It should be note that the SaskPower Boundary Dam project in Canada is the world's first commercial-scale post-combustion coal-fired carbon capture and storage project, and was started in September 2014, using the CO_2 for EOR in the Weyburn oil field [32].

Respect to alternatives to mitigate CO_2 emissions from both power sector and energy-intensive industrial processes, partial oxy-combustion is considered a promising CCS technology that can potentially minimize the energy requirements of the overall CO_2 capture process provided above. This hybrid technology combines an oxygen-enriched air combustion followed by a CO_2 separation process from an elevated CO_2 concentrated flue gas by typically means of chemical absorption. Favre et al. suggest a minimal energy consumption around 40%v/v - 60%v/v O_2 concentration in the oxidizer that can lead to 25% reduction compared with conventional CCS technologies [33, 34]. Previous works demonstrated the benefits that partial oxy-combustion provided in the CO_2 separation stage, strengthening the CO_2 absorption process based on chemical absorption. In particular, the presence of more CO_2 in the flue gas enhanced the absorption rates and also increased the CO_2 loading of the rich amine after the CO_2 absorption

stage [35]. In addition, the use of higher CO_2 concentrations in the flue gas decrease the oxidative degradation of amine-based solvents [36, 37].

Several authors realized a techno-economic evaluation of the overall CCS technology based on partial oxy-combustion [34, 38, 39]. Recently, Cau et. al. published a techno-economic analysis of a 1000 MWth partial oxy-combustion plant based on an ultra-supercritical pulverized coal combustion power plant integrated with a post-combustion CO_2 capture system. This work was supported by simulation models, particularly Aspen Plus™ and Gate Cycle™. Cau concluded that partial oxy-combustion was not feasible from the economic point of view in comparison with oxy-combustion using high purity O_2 as oxidizer. This work, and also the study from Huang [39], proposed a partial O_2-fired combustion based on the use of a high purity O_2 combined with air. The production of O_2-enriched air is not considered in these works. In addition, Cau estimated a slightly reduction of the CO_2 capture and compression step, from 32.4 MW (post-combustion case) to 30.4 MW (partial oxy-combustion 90% high purity O_2 – 10% air). The CO_2 capture costs for partial oxy-combustion varied from 40.35 €/t CO_2 to 25.42 €/t CO_2 whereas the oxy-combustion case resulted in 22.81 €/t CO_2. The advantages of partial oxy-combustion in terms of significant decrease of the energy requirements in the solvent regeneration process should be explore the possibilities that partial oxy-combustion has to avoid the above-mentioned CO_2 capture cost gap. Finally, most of the studies focused on CO_2 concentrations in the flue gas derived from conventional fossil-fuel combustion, typically ranging between 3%v/v – 15%v/v CO_2. Results from either pilot plant or lab rig tests at CO_2 concentrations above 15%v/v have not been established yet. Therefore, further investigations using higher CO_2 concentrated flue gases are required to evaluate the performance of CO_2 chemical absorption under partial oxy-combustion conditions.

2. CO_2 lab-scale plant description

The experimental CO_2 capture lab-scale plant is based on a reversible chemical absorption process. It was designed to operate in a wide range of CO_2 flue gas compositions that should represent the variety of CO_2 capture processes can be tested in this installation. In particular, the synthetic flue gas simulates treated exhaust gases derived from the conventional fossil-fuel combustion process to the oxygen-enriched air fossil-fuel combustion process, namely partial oxy-combustion. The CO_2 content in the flue gas treated during partial oxy-combustion operations was set in the range 15%v/v-60%v/v. CO_2 concentrations over 60%v/v CO_2 would be close to the flue gas composition derived from a conventional oxy-combustion process (80%v/v-90%v/v CO_2) and, therefore, it might be not economically feasible [30].

Table 1. Main characteristics of the absorber and stripper units

Absorber	
Temperature (°C)	50
Operating pressure (bara)	1
ID (mm)	30
Column material	borosilicate glass
Random packing	Raschig rings 6 mm
Packing material	Ceramic
Packing height (m)	0.7
Number of packing beds	4
Stripper	
Temperature (°C)	120
Operating pressure (bara)	2
Electrical power (W)	750
ID (mm)	25
Column material	316L
Random packing	Raschig rings 6mm
Packing material	316L
Packing height (m)	0.7
Number of packing beds	2

The CO_2 capture bench-scale plant is described in detail below. It consists of two random packed columns comprising the absorber and the stripping units. The columns have an internal diameter (ID) of 30 mm and 25 mm and they were filled using ceramic and stainless steel 316L 6 mm

raschig rings. The height of the packing beds can be varied from 0.7 m to 3 m and from 0.7 m to 1.4 m in the absorber and the stripper, respectively.

As it can be seen in Table 1, the operating conditions are similar to conventional post-combustion capture operations using flue gas derived from conventional pulverized-coal power plants. A scheme of the experimental CO_2 bench-scale plant is represented in Figure 1. The synthetic flue gas is provided by a set of cylinders containing CO_2 and N_2. Two mass-flow controllers adjust the desired gas composition. After the synthetic flue gas is provided, it is conditioned before entering the CO_2 absorption section. The synthetic flue gas is then passed through the gas conditioning system, where it is heated at the desired temperature and it is also saturated prior to being introduced into the absorber, as illustrated in Fig. 1.

A thermostatic bath filled with thermal oil and an immersion thermostat are employed to set the absorption temperature. The synthetic flue gas passes through a 4-mm stainless steel coiled tube which is totally immersed into the thermal oil. After that, the heated flue gas is introduced into an impinger filled with deionized water to saturate the flue gas stream. This impinger is also placed into the thermostatic bath to maintain the operating temperature constant as the saturation process occurs. The synthetic flue gas conditions are set at conventional absorption temperature, ranging between 40°C and 60°C, and ambient pressure. A gas sampling port is used after the N_2/CO_2 mixing to facilitate a preliminary verification of the flue gas composition.

After flue gas conditioning, the synthetic flue gas is then introduced into the absorption unit, where it is put in contact with the lean solvent countercurrent. A 90% of CO_2 capture efficiency is achieved in this unit. The absorber temperature profile is measured during the experiments using five pt-100 temperature sensors set below each packing bed and the demister. The differential pressure connected between the bottom and the top of the absorber is also measured using a differential pressure transducer. Finally, the cleaned exhaust gas leaves the absorber from the top and is then cooled using a coil refrigerant and dried by means of an

impinger filled with silica gel prior to being sent to a safe place. A gas aliquot of 1.5 mL/min is taken to determine the CO_2 concentration using a FTIR- CO_2 analyser (Testo™ XL model 350 XL) and, therefore, the CO_2 capture efficiency during the experiments.

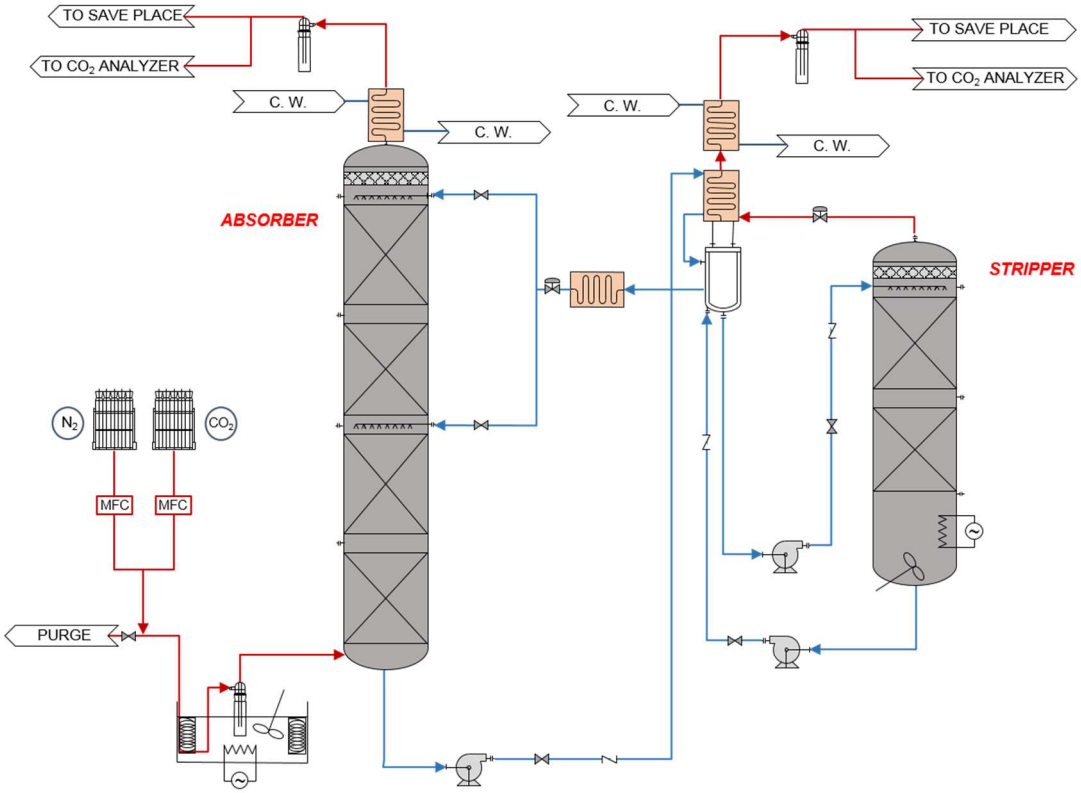

Figure 1. Basic scheme of the CO_2 bench-scale plant

The CO_2 is transferred from the gas phase to the solvent in contact with the flue gas along the absorber. The rich amine containing the absorbed CO_2 is extracted from the bottom of the absorber column and is pumped to the lean-rich amine heat exchanger using a variable speed peristaltic pump. Liquid samples can be withdrawn for CO_2 loading determinations from the liquid sampling ports placed along the absorber and before the peristaltic pump inlet. The rich solvent is heated from the bulge temperatures - around 65-70°C - to 100°C before entering the stripping unit. A heat exchanger uses the heat from the CO_2 exhaust gas from the stripper and the lean-rich amine heat exchanger employs the lean amine leaving the stripper to heat the rich solvent.

A second peristaltic pump is used to send the heated rich amine from the lean-rich amine hear exchanger bottom to the stripping inlet. An electrical heating device supplies the energy required for CO_2 release and water vapour stream generation. The power supply to the electrical heating device is controlled by a PID controller, which sets the desired bottom temperature of the stripper. The stripper pressure is also controlled using a pressure switch that maintains the desired operating pressure acting on the solenoid valve installed at the top of the stripper. Finally, three K-thermocouples measure the temperature profile along the stripper and a variable speed agitator with a speed controller is used to stir the solvent placed at the stripper bottom. As occurred with the absorber, the stripper can be fed at different positions from two inlets at the top of each packing bed.

3. Materials and methods

Monoethanolamine (MEA) is considered the benchmark for CO_2 capture based on chemical absorption [22,23]. A 30wt% MEA aqueous solution was tested as a solvent in this work. MEA was supplied by Acros Organics with 99 vol.% purity. For the gas phase, CO_2 and N_2 cylinders were supplied by Linde™ to provide the synthetic flue gas under different compositions.

The operation of the CO_2 capture bench-scale unit is described in detail. The post-combustion case was set using 7 L/min of synthetic flue gas containing 15%v/v CO_2. Two experiments were run using two and four packing beds in the absorber. As it was indicated in Table 1, the operating conditions of the CO_2 capture bench-scale unit were within typical operating conditions for post-combustion capture units applied to pulverized coal power plants from CO_2 capture pilot plant operations: absorption temperature 50˚C, stripping temperature 120˚C, stripping pressure 2 bara. The L/G ratio was adjusted by varying the solvent flow-rate until a 90% capture efficiency was achieved. A comprehensive evaluation of the CO_2 capture bench-scale unit performance under partial oxy-combustion conditions using MEA 30wt% were performed with 38 experiments run summarized in Tables 2 and 3. Three levels of CO_2 composition of the flue gas

were studied using two and four random packing beds, as it occurred in post-combustion runs. According to Favre et al. [33], the minimal separation work considered as a trade-off between the O_2 separation for O_2-enriched air production and the CO_2 separation from the flue gas produced during the O_2-enriched air combustion is found below 60%v/v O_2 in the oxidizer. To ensure the evaluation of the optimal range in which partial oxy-combustion might be economically feasible compared with both post-combustion and oxy-combustion, a 75%v/v O_2 in the oxidizer was set as a maximum O_2-enrichment. Higher O_2 concentrations were found out of the optimal range for the minimal separation work and they were not considered further in this work. The combustion process of a conventional pulverized coal boiler using a 75%v/v O_2 in the oxidizer led to produce a 60%v/v CO_2 concentration in the flue gas that was consistent with flue gas compositions derived from oxy-combustion process using high purity O_2, ranging between 80-90%v/v CO_2 [9]. Therefore, 60%v/v CO_2 was the highest CO_2 concentration studied in this work.

A wide range of L/G ratios were studied to determine the optimal L/G ratio that can provide the lowest energy requirement during solvent regeneration process at each flue gas composition. The L/G ratio should be higher as the CO_2 content in the flue gas increases.

Table 2. Partial oxy-combustion test campaign

RUN	Reference number	Stripper Pressure (bara)	Tstrip (°C)	$[CO_2]g$ (%v/v)	L/G Ratio (kg/kg)	Random Packing Beds
#1.1	MEA - 20 – 1.5	2	120	20	1.5	2
#1.2	MEA - 20 - 5				5	
#1.3	MEA - 20 – 6.5				6.5	
#1.4	MEA - 20 - 8				8	
#1.5	MEA - 40 - 3			40	3	
#1.6	MEA - 40 - 5				5	
#1.7	MEA - 40 - 8				8	
#1.8	MEA - 40 - 10				10	
#1.9	MEA - 40 - 12				12	
#1.10	MEA - 40 – 13.2				13.2	
#1.11	MEA - 60 - 10			60	10	
#1.12	MEA - 60 – 13.2				13.2	
#1.13	MEA - 60 - 16				16	
#1.14	MEA - 60 - 18				18	
#1.15	MEA - 60 - 20				20	
#1.16	MEA - 20 – 1.5 (4)	2	120	20	1.5	4
#1.17	MEA - 20 - 5 (4)				5	
#1.18	MEA - 20 – 6.5 (4)				6.5	
#1.19	MEA - 20 - 8 (4)				8	
#1.20	MEA - 40 - 3 (4)			40	3	
#1.21	MEA - 40 - 5 (4)				5	
#1.22	MEA - 40 - 8 (4)				8	
#1.23	MEA - 40 - 10 (4)				10	
#1.24	MEA - 40 - 12 (4)				12	
#1.25	MEA - 40 – 13.2 (4)				13.2	
#1.26	MEA - 60 - 10 (4)			60	10	
#1.27	MEA - 60 – 13.2 (4)				13.2	
#1.28	MEA - 60 - 16 (4)				16	
#1.29	MEA - 60 - 18 (4)				18	
#1.30	MEA - 60 - 20 (4)				20	

Six verification tests were run to confirm the feasibility of the optimal L/G ratio established in the previous experiments reported in Table 2. In those experiments, the operating conditions were reproduced for each flue gas composition using the optimal L/G ratio that led to a minimal

energy requirement during the CO_2 stripping process. Table 3 summarizes the operating conditions for the verification tests carried out.

Table 3. Verification tests for the optimal L/G determinations during the MEA test campaign

RUN	Reference number	Stripper Pressure (bara)	Tstrip (°C)	$[CO_2]g$ (%v/v)	L/G Ratio (kg/kg)	Random Packing Beds
#1.31	MEA - 20 - OPT (2)	2	120	20	*Optimum determined by polynomial approximation	2
#1.32	MEA - 40 - OPT (2)			40	*Optimum determined by polynomial approximation	
#1.33	MEA - 60 - OPT (2)			60	*Optimum determined by polynomial approximation	
#1.34	MEA - 60 - OPT (2)*			60	*Optimum determined by polynomial approximation	
#1.35	MEA - 20 - OPT (4)			20	*Optimum determined by polynomial approximation	4
#1.36	MEA - 40 - OPT (4)			40	*Optimum determined by polynomial approximation	
#1.37	MEA - 60 - OPT (4)			60	*Optimum determined by polynomial approximation	
#1.38	MEA - 60 - OPT (4)*			60	*Optimum determined by polynomial approximation	

Each experiment requires two hours' mean average stabilization time to reach the steady-state condition. The experiments last three hours, maintaining stable conditions to determine the average values of the representative parameters of the CO_2 absorption process. Based on the operational procedure described above, all the experiments were run twice in order to verify the experimental results, which were found within ±5% of accuracy in comparison between both runs. The experimental results were the mean average values from the two experiments run at the same operating conditions. The experimental results were the mean average values from

the two experiments run at the same operating conditions. The data recording of the most relevant parameters is carried out along the steady-state of each experiment following the procedure described in detail below:

1. Continuous data acquisition: Density, temperature and flow-rate of the lean solvent with the CO_2 concentration of the cleaned gas are recorded continuously throughout the experiments and they are stored in the PC.
2. Liquid samples are withdrawn at intervals of 30 minutes to determine the CO_2 loading of the lean and rich amine using the above-mentioned TOC analyzer. These measurements allow to calculate the CO_2 cyclic capacity during each experiment.
3. Data is recorded at intervals of 30 minutes to evaluate the evolution of each parameter during the experiments. These data are used to determine the main target parameters: the CO_2 capture removal efficiency, using Eq. 1, and the specific energy consumption in the stripper using the Eq. 2:

$$CO_2\ removal\ efficiency\ (\%) = \frac{\dot{m}_{CO2IN} - \dot{m}_{CO2OUT}}{\dot{m}_{CO2IN}} * 100 \qquad \text{(Eq. 1)}$$

Where, '$\dot{m}_{CO2}$ ' and '$\dot{m}_{CO2OUT}$' denote the CO_2 mass-flow rates from the flue gas at both the inlet and the outlet of the absorber, expressed in kg/s.

$$Spec\ Ener\ Cons\ \left(\frac{GJ}{tCO_2}\right) = \frac{\frac{[P_F - P_I]}{t_{min}/60} * 10^{-6}}{Q_{fg} * [CO_2]_{IN} * \bar{\zeta}_{capture} * \rho_{CO_2} * 10^{-6}/60} \qquad \text{(Eq. 2)}$$

Where, 'P_F' denotes de total energy consumed at the end of the measurement interval, expressed in kWh. 'P_I' denotes de total energy loss during the experiments expressed in kWh.

The energy loss was calculated following the procedure described by Notz et. al. This parameter takes into account the heat losses from two main equipment of the installation - the lean-rich amine heat exchange and the stripper – and the heat loss of the rich amine stream from the absorber outlet to the stripper inlet [22]. 't_{min}' represents the interval time expressed in min, typically 30 minutes. 'Q_{fg}' denotes the gas flow-rate expressed in L/min. '$[CO_2]_{IN}$' denotes the CO_2 concentration in the flue gas at the absorber inlet, expressed in %v/v. 'η_{capure}' denotes the CO_2 capture efficiency obtained in the experiment. 'ρ_{CO2}' denotes the CO_2 density at ambient temperature expressed in g/L.

According to Notz et. al. [22], there are unavoidable heat losses, particularly in small plants, that overestimate the specific energy consumption related to the solvent regeneration. In all the cases, the heat losses determined were found below 30% of the total heat duty supplied to the reboiler, which were in accordance with the Notz´s heat loss determinations – 29.9% and 28.7% of the total heat duty. Therefore, we removed the heat losses calculated in the bench-scale unit for the total heat duty supplied for the specific energy consumption determination in each experiment [22].

The bench-scale CO_2 capture unit was modelled using Aspen Plus™ based on the flow diagram plotted in Fig. 1 in order to compare and validate the main insights extracted from the experimental results obtained after the execution of the test campaign [40]. The electrolyte-NRTL model was used for modelling the vapor-liquid equilibrium and the reaction kinetics of the MEA-CO_2-water system was based on previous work from Little et. al. [41].

4. Results

The MEA 30wt% test campaign was focused on the combination of MEA with partial oxy-combustion capture process and also on its comparison with a conventional post-combustion capture. The results have been divided into five sub-sections that are set out below, in which

the influence of the most relevant operating parameters on the performance of the bench-scale plant has been studied. The elevated number of runs has provided a robust characterization of the unit performance and feasibility, as shown by the limitations of the major operating ranges.

4.1 Effect on the absorber temperature profiles

In general, the temperature bulge location defines the absorber zone where most of the CO_2 is absorbed. In addition, the optimum operational L/G ratio is often found to close to the value that provides the maximum temperature bulge. Figure 2 represents the absorber temperature profiles from both the post-combustion case and the experiments involving 20%v/v CO_2.

The absorption performance can be adequately evaluated from the temperature profiles along the absorber. Respect to the post-combustion run (baseline case), the temperature profiles showed similar behaviour to those obtained from the experimental installation referenced in the literature [22, 23, 42, 43]. The differences observed in the measurements of the absorber temperature profile for each experiment run at the same conditions were below 1˚C. The temperature increased from the absorber top, where most of the CO_2 absorption occurred. The temperature bulge was 44.7 °C in this run and it was reached in the first meter of packing from the absorber top. From this point, the temperature decreased until the flue gas inlet at the absorber bottom where the flue gas was introduced at 50˚C. The heat associated to the CO_2 solubility enthalpy is mainly released at the absorber top where the temperature bulge located, producing such temperature increase in the absorber. The CO_2 mass transfer from the bulk gas to the liquid gas occurred mainly in this section of the absorber, being limited in the down section of the absorber. For this reason, the heat released due to the absorption of the CO_2 by MEA decreased in this section because the CO_2 absorbed was lower compared to the absorber top. The CO_2 solubility enthalpy was not able to balance the heat losses along the absorber with the environment, producing the decrease of the temperature profile observed in the baseline case plotted in Fig. 1. Finally, a temperature increase was observed due to the sensible heat

supplied by the flue gas introduced at 50°C from the absorber bottom. In partial oxy-combustion runs, the temperature profiles exhibited a similar trend as the post-combustion run, particularly the runs set at L/G ratio 5 and L/G ratio 6.5 (Fig. 2). The highest temperature bulge obtained from these experiments was 44.6 °C, similar to those provided by the post-combustion case. An increase of the L/G ratio produced that the absorption of CO_2 occurs further down in the absorber and the temperature bulges, therefore, shifted closer to the absorber bottom, as it can been seen from the L/G ratio 5 and L/G ratio 6.5 curves plotted in Fig. 2. In the experiments set with an elevated L/G ratio - over 6.5 -, the presence of higher amounts of solvent inside the absorber limited the increase of the temperature profile. The temperature bulge was 40.2˚C and was located at the absorber bottom. The heat associated to the CO_2 solubility enthalpy released was not able to balance the heat losses along the absorber and neither to increase the temperature of the higher amount of solvent. The temperature profile showed a linear behaviour with lower temperatures along the absorber compared with lower L/G ratio experiments, as the L/G ratio 8 curve illustrates in Fig. 2. Temperature profiles calculated from the simulation model were found within ± 5˚C compared with the experimental results (Fig. 2), showing similar accuracy than others experimental tests combined with process simulation studies in CO_2 capture via chemical absorption [25].

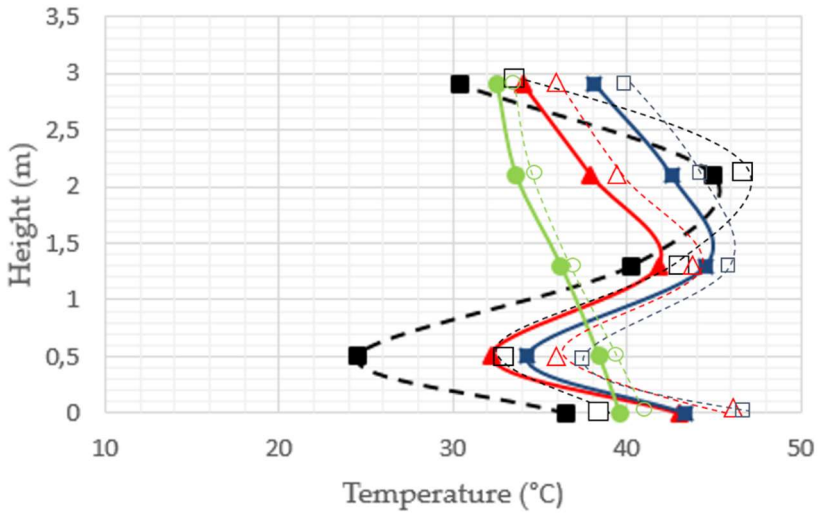

Figure 2. Absorber temperature profiles from experiments set with four packing beds: post-combustion exp. (▬ ■ ▬) and 20%v/v CO_2 cases setting L/G ratio 5 (—■—); L/G ratio 6.5 (—■—) and L/G ratio 8 (—●—). Empty markers represent temperature profiles from the simulations performed under the same operating conditions than full markers.

The above-mentioned effect was also observed at higher CO_2 concentrations, as seen in Fig. 3. Experiments set with lower L/G ratios, from 3 to 8, increased their temperatures progressively along the absorber. In those runs, the temperature bulges also moved down in the absorber as L/G ratio increased. That effect occurred due to the fact that a higher amount of CO_2 has to be absorbed in 40%v/v CO_2 experiments in comparison with the post-combustion case and thereby a higher L/G ratio is required to achieve elevated CO_2 removal. The maximum temperature bulge was 49.2°C and was obtained for L/G ratio 8. It should be noted that a higher temperature bulge was obtained compared to the post-combustion run since a higher amount of absorbed CO_2 balanced the higher L/G ratio required. From the L/G ratio 8 experiment, the excess of solvent flow-rate forced the temperature bulge to move down towards the absorber bottom, whereas lower temperatures were reached progressively as higher L/G ratios were utilized.

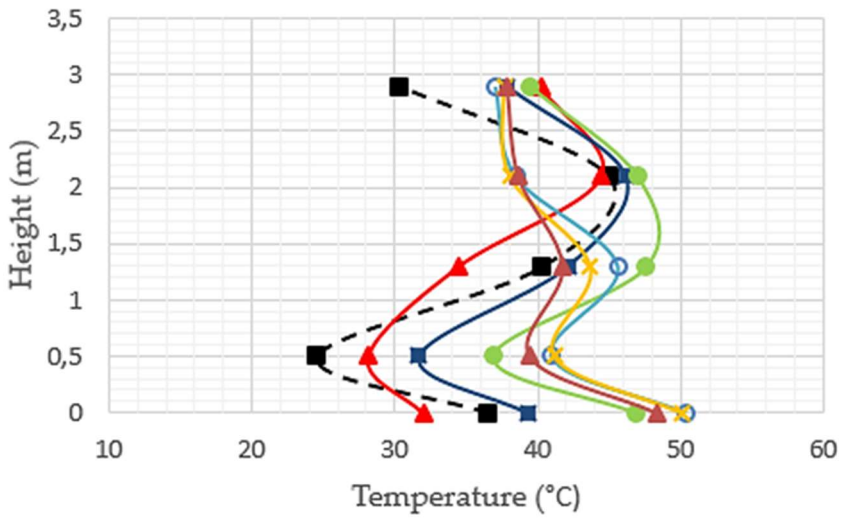

Figure 3. Absorber temperature profiles obtained from experiments set with four packing beds: post-combustion (▬ ■ ▬) and 40%v/v CO_2 setting L/G ratio 3 (—▲—); L/G ratio 5 (—■—); L/G ratio 8 (—●—); L/G ratio 10 (—○—); L/G ratio 12 (—✕—) and L/G ratio 13.5 (—▲—)

4.2 Effect on the stripping temperature profiles

The temperature profiles of the stripper for each experiment were also analysed. Figure 4 summarizes the temperature profiles of the experiments using 40%v/v CO_2 and four packed beds. The variations on the measurements of the stripper temperature profile for each experiment run at the same conditions were ± 1˚C.

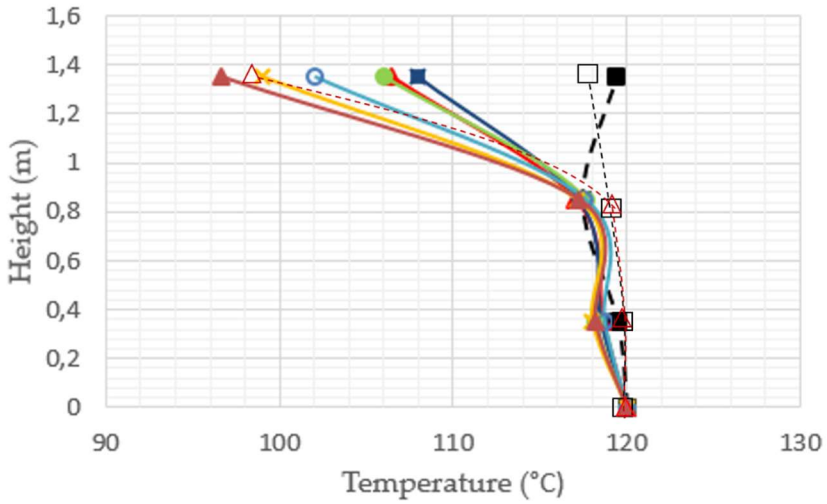

Figure 4. Stripper temperature profiles obtained from experiments set with four packing beds: post-combustion (▬ ■ ▬) and 40%v/v CO_2 setting L/G ratio 3 (—▲—); L/G ratio 5 (—■—); L/G ratio 8 (—●—); L/G ratio 10 (—○—); L/G ratio 12 (—✕—); L/G ratio 13.5 (—▲—). Empty markers represent temperature profiles from the simulations performed under the same operating conditions than full markers.

The post-combustion run showed a homogenous temperature along the stripper, with values close to 120°C. Unlike in the post-combustion case, the partial oxy-combustion experiments offered a significant temperature variation along the stripper, mainly located at the top of the column. The higher the L/G ratio, the lower the temperature at the stripper top. Higher L/G

ratios were produced by an increase of the solvent flow-rate that constrained the heat transfer between the hot lean amine leaving the stripper and the cold rich amine leaving the absorber. Higher solvent flow-rates had influence on the residential time in lean-rich amine coiled heat exchanged, reducing the temperature of the rich amine stream before entering the stripper and hence the temperature at the stripper top decreased in every experiment. Although L/G ratio variations influenced the temperature profiles of the stripper, they had a slight effect on the stripper performance in terms of CO_2 loading of the lean amine, which was further discussed in next section. However, a specific design of the lean-rich amine heat exchange is recommended for a particular partial oxy-combustion operation to avoid this limitation. Temperature profiles of the stripper determined from the simulation model were found within ± 2˚C compared with the experimental results (Fig. 4).

4.3 Effect on the CO_2 cyclic capacity

The CO_2 cyclic capacity was studied by means of the CO_2 loading determinations for both the lean and rich solvent during each experiment. As it can be observed from Figure 5, the L/G ratio had a minimal influence on the CO_2 loading of the lean amine leaving the stripper. Only a slight increase on the CO_2 loading was observed as L/G ratio increased. The CO_2 loading of the lean amine was ranging between 0.13 and 0.15 mole CO_2 per mole solvent in all the partial oxy-combustion experiments (Fig. 5). This may occur due to the fact that a higher L/G ratio reduced the resident time of the rich solvent inside the stripper and the solvent regeneration could not reach the CO_2 desorption level achieved, i.e., in the post-combustion run.

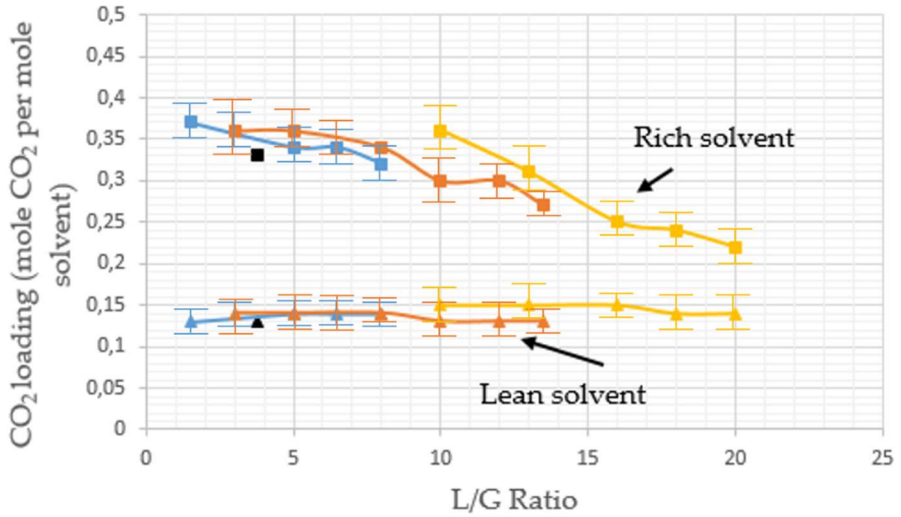

(a)

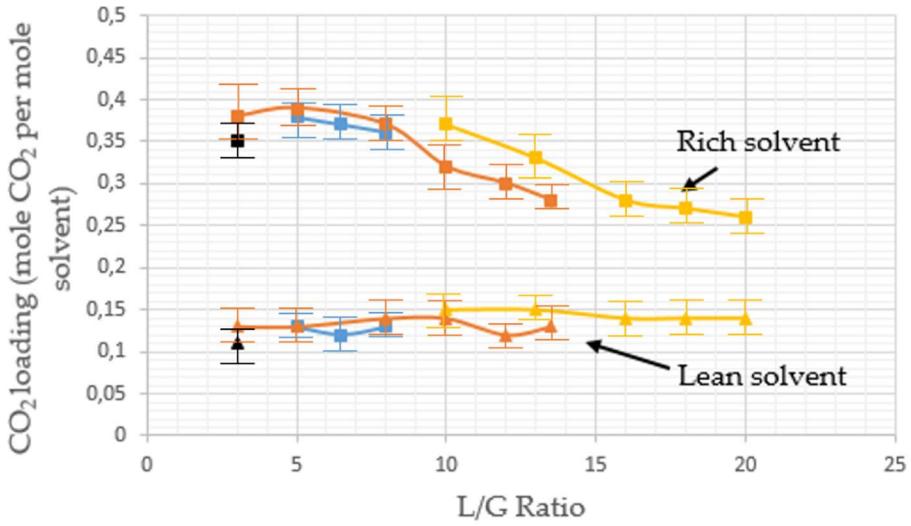

(b)

Figure 5. CO_2 loading evolution of lean and rich amine as function of L/G ratio. (a) two packed beds experiments, (b) four packed beds experiments. Square dots represent rich solvent loadings and triangles represent lean solvent loadings. The markers and lines represent: post-combustion rich solvent (■), post-combustion lean solvent (▲), 20%v/v CO_2 (—), 40%v/v CO_2 (—) and 60%v/v CO_2 (—)

On the contrary, L/G ratio had a significant impact on the rich amine loading and hence on the CO_2 cyclic capacity. Higher L/G ratios produced lower CO_2 loadings of the rich amine and also lower cyclic capacity on the overall solvent performance, as illustrated in Fig. 5. The CO_2 loadings of the rich amine were progressively decreased from values close to 0.40 mole CO_2 per mole

solvent at 20%v/v CO_2 to 0.25 mole CO_2 per mole solvent at 60%v/v CO_2 as a result of the elevated L/G ratios required to get a particular CO_2 removal as CO_2 concentration was higher. Even though the presence of higher CO_2 content in the flue gas often led to higher CO_2 loading of the solvent, the elevated solvent flow-rate needed for a certain CO_2 removal efficiency resulted in a lower CO_2 loaded rich solvent. In addition, the results confirmed that the CO_2 cyclic capacity of the solvent and the CO_2 loading levels were higher in all experiments using four packed beds instead of two packed beds, showing a slight enhancement of the overall CO_2 capture process. It is clear that a specific design of the CO_2 capture plant must be performed for a defined partial oxy-combustion operation to maximize the feasibility and the performance of the CO_2 capture process.

4.4 Effect on the CO_2 removal efficiency

The evaluation of the overall performance of the CO_2 capture plant under partial oxy-combustion conditions was analysed from the point of view of CO_2 removal efficiency. Figure 6 represents the CO_2 removal efficiency as a function of L/G ratio at both different CO_2 concentrations and varying packed bed heights. The variations of the CO_2 concentration measurements in the exhaust gas were below 1% for the two experiments run at the same conditions. As it can be seen in this figure, higher L/G ratios were required for elevated CO_2 concentration experiments to achieve similar (or more) CO_2 capture efficiency than the post-combustion case (90%), shifting the curves towards the right side region. In particular, the post-combustion case required L/G ratios of around 4 to achieve efficiencies over 90%, whereas experiments carried out at 40%v/v CO_2 needed L/G ratios over 10 to achieve more than 90% CO_2 capture efficiency using MEA 30wt%. In the experiments set at 40%v/v CO_2, a 94% of CO_2 removal efficiency was achieved with an L/G ratio of 12.

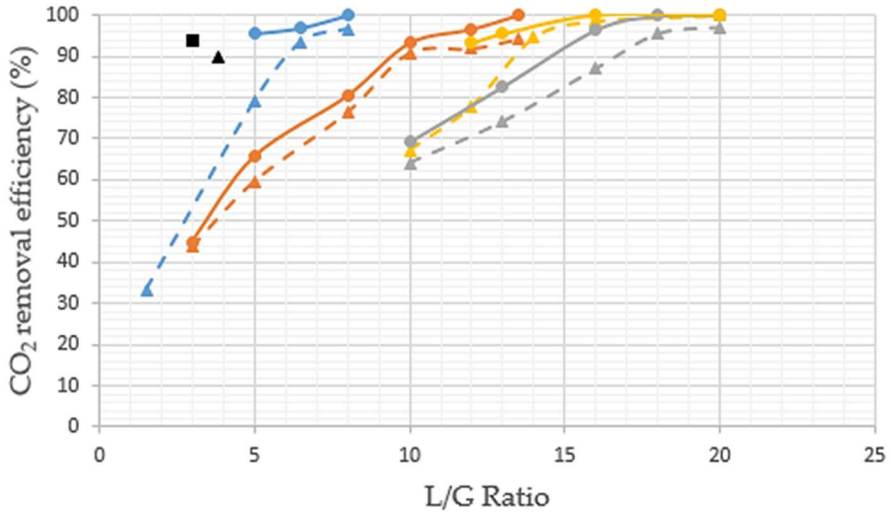

Figure 6. CO_2 capture efficiency plotted versus L/G ratio. Dashed lines represent two packed bed experiments whereas continuous lines represent four packed bed experiments. The markers and lines represent: post-combustion four packed beds (■), post-combustion two packed beds (▲), 20%v/v CO_2 (—), 40% v/v CO_2 (—), 60% v/v CO_2 (—) and 60% v/v CO_2 using fresh amine (—).

To obtain the same efficiency, 60%v/v CO_2 cases (grey lines in Fig. 6) required L/G ratios of 14.5 (4 beds) and 17 (2 beds), respectively. The 60%v/v CO_2 experiments were also run using amine make-up which replaced the solvent utilized in 20%v/v and 40%v/v experiments. These experiments were plotted with yellow lines in Fig. 6. A significant enhancement of the solvent performance was observed in comparison with cases in which there was no amine replacement. When four packed beds were utilized, all the experiments that used fresh solvent resulted in CO_2 capture efficiencies over 90%. As discussed above, the experiments carried out using four packing beds exhibited higher efficiency compared with two packing beds for all the runs.

4.5 Effect on the reboiler duty

The most promising results related to partial oxy-combustion operation were revealed once the reboiler duty requirements were evaluated for the MEA 30wt% experiments. Figure 7 shows the specific energy consumption in the stripper unit expressed as GJ per tonne of captured CO_2 as a

function of the L/G ratio. As it can be extracted from the results plotted in this figure, a CO_2 capture process based on partial oxy-combustion operation using MEA 30wt% provided a huge reduction of the energy requirements during the desorption process. In particular, a 30% reduction was achieved using 20%v/v CO_2 in flue gas in comparison with the reference case (post-combustion). Reductions around 45% and 55% were also achieved using a flue gas composition of 40%v/v and 60%v/v CO_2, respectively. Indeed, the reduction was as much as 60% when the amine make-up was combined with 60%v/v CO_2. As occurred above, improvements in the overall CO_2 capture performance were obtained when four packing beds were used instead of two packing beds.

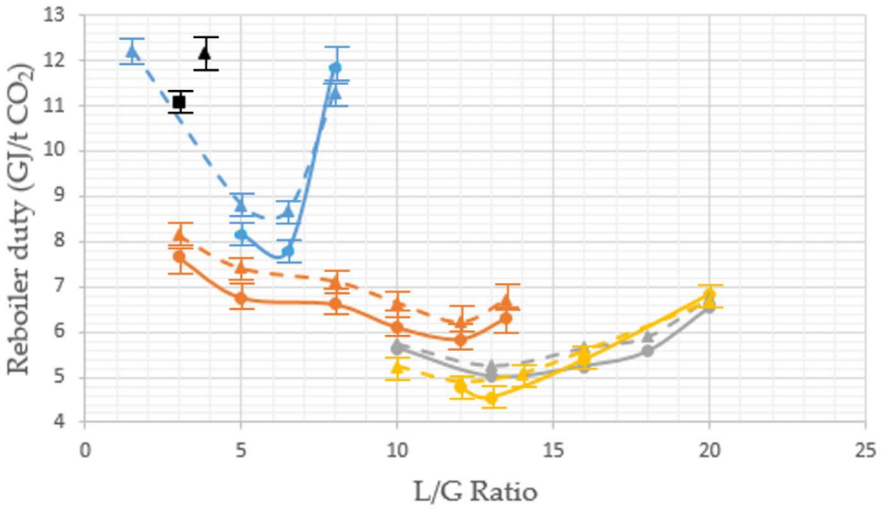

Figure 7. Specific energy consumption in the stripper versus L/G ratio. Dashed lines represent two packed beds experiments whereas continuous lines represent four packed bed runs. The markers and lines represent: post-combustion four packed beds (■), post-combustion two packed beds (▲), 20%v/v CO_2 (—), 40% v/v CO_2 (—), 60% v/v CO_2 (—) and 60% v/v CO_2 using fresh amine (—).

The optimal L/G ratios that can lead to the highest reduction of the specific energy requirements of the CO_2 capture process for each CO_2 composition were estimated from the curves plotted in Fig. 7 using polynomial approximations. The CO_2 removal efficiency associated with those values were also calculated from the curves represented in Fig. 6. The calculations were summarized in

Table 4. The optimal L/G ratios were run at the bench-scale plant to verify the estimations made from the experimental results. As can be seen in Table 4, the specific energy consumptions experimentally determined were within 5% of the values obtained using the polynomial approximation and 10% of these provided by Aspen Plus™ simulations, although the experimental results were higher than the previous estimations in terms of specific energy requirement.

Table 4. Summary of the optimal L/G ratios determined by polynomial approximation and the verification test results during the MEA test campaign.

	Polynomial approximation results			Simulation results			Experimental results		
Run	Capture Removal (%)	Reboiler Duty (GJ/t CO_2)	L/G ratio	Capture Removal (%)	Reboiler Duty (GJ/t CO_2)	L/G ratio	Capture Removal (%)	Reboiler Duty (GJ/t CO_2)	L/G ratio
Post-combustion (2)	-	-	-	90.0	11.31	2.8	89.8	12.18	3.8
MEA-20-OPT (2)	88.7	8.47	5.9	85.0	8.44	5.6	85.2	8.56	6.0
MEA-40-OPT (2)	93.0	6.18	11.8	90.0	6.23	11.1	90.9	6.36	11.8
MEA-60-OPT (2)	75.9	5.17	13.2	75.0	5.27	10.3	75.3	5.38	13.3
MEA-60-OPT (2)*	82.1	4.81	12.3	85.0	4.87	11.6	83.3	4.98	12.5
Post-combustion (4)	-	-	-	90.0	10.16	2.6	94.0	11.10	3.0
MEA-20-OPT (4)	96.1	7.41	5.9	95.0	7.02	5.4	96.0	7.61	6.0
MEA-40-OPT (4)	96.8	5.78	11.9	95.0	5.58	10.9	95.7	5.88	12.0
MEA-60-OPT (4)	88.2	5.00	14.1	85.0	5.07	10.1	86.4	5.13	14.2
MEA-60-OPT (4)*	95.9	4.55	13.2	95.0	4.68	11.5	95.7	4.74	13.3

* referring to experiments using amine make-up at 60%v/v CO_2

All the values determined in this work regarding the specific energy consumption during the regeneration stage are consistent with previous work using MEA. Tobiesen et al. [44] obtained a specific energy requirement of 3.7 – 10.2 GJ per tonne CO_2 whereas Dugas [45] reported values in the range 5.1 – 14.2 GJ per tonne CO_2. These works operated under similar conditions in terms of stripping pressure – 2 bara and 1.6 bara – and CO_2 loading of the lean amine – 0.22 – 0.41 mole CO_2 per mole solvent and 0.14 – 0.37 mole CO_2 per mole solvent.

The lowest energy requirements were obtained from experiments using 60%v/v CO_2. They also exhibited further improvements in cases where solvent make-up was used. It should be noted that the maximum reductions achieved in the testing were 59.1% and 57.3% in comparison with the post-combustion cases using two packing beds and four packing beds, respectively.

In this respect, the four packing bed experiments improved the CO_2 absorption performance in all cases in comparison with the two packing bed experiments. Although the optimal L/G ratios were moved to higher values, they also achieved CO_2 removal efficiencies over 95% and lower energy requirements, below 5 GJ/t CO_2, according to experimental determinations. In 60%v/v CO_2 experiments, the four packing bed experiments provided the lowest specific energy requirement - 4.74 GJ/t CO_2 - that supposed a 57.3% of reduction compared with the post-combustion baseline case.

According to Cau et. al., the maximum energy reductions achieved for partial oxy-combustion were 6.2% and 43.1% compared to post-combustion and oxy-combustion, respectively. However, the oxy-combustion configuration provided the lowest CO_2 capture cost. The evaluation of partial oxy-combustion provided an 11% CO_2 capture cost increase for the most promising partial oxy-combustion case. The reductions on the energy requirements for the CO_2 separation process determined in this work – over 50% in some experiments - might balance the energy consumption associated to the O_2-enriched air production. It also could decrease the

above-mentioned CO_2 capture cost gap and even make partial oxy-combustion more feasible than oxy-combustion for CCS applied to power plants.

5. Conclusions

A CO_2 capture bench-scale unit was used to evaluate the behaviour of MEA 30wt% under partial oxy-combustion operation. 38 experiments were performed in order to study the effects that variations on the CO_2 concentration in the flue gas had on the main operating parameters of a regenerative CO_2 chemical absorption process such as temperature profiles, CO_2 cyclic capacity, CO_2 removal efficiency and specific energy consumption during the regeneration step. The use of a more CO_2 concentrated flue gas required higher L/G ratios to achieve CO_2 removal efficiencies over 90%. The increase of the L/G ratios resulted in lower temperature profiles along the absorber and hence the temperature bulges also moved down in the absorber. The same effect was observed in the stripping temperature profiles. The partial oxy-combustion experiments offered a significant decrease of the temperature at the stripping top. The higher the L/G ratio, the lower the temperature at the stripper top. However, the decrease of the stripping temperature profile had a slight influence on the CO_2 loading of the lean amine, which was kept almost constant, ranging between 0.13 and 0.15 mole CO_2 per mole solvent, in all the partial oxy-combustion experiments. On the contrary, the CO_2 loadings of the rich amine were progressively decreased from values close to 0.40 mole CO_2 per mole solvent at 20%v/v CO_2 to 0.25 mole CO_2 per mole solvent at 60%v/v CO_2 as a result of elevated L/G ratios that implied lower resident time in the absorber. The CO_2 removal efficiency required higher L/G ratios once elevated CO_2 concentration was set to achieve 90% of CO_2 capture efficiency. The operation under partial oxy-combustion conditions of a chemical absorption based on MEA 30wt% provided a huge reduction of the energy requirements during the desorption process. In particular, a 30% reduction was achieved using 20%v/v CO_2 in flue gas in comparison with the reference case (post-combustion). The lowest specific energy requirement was achieved using

60%v/v CO_2 where the energy requirement for the regeneration stage was 4.74 GJ/t CO_2. This value implied a decrease of 57.3% of the heat duty compared with the post-combustion baseline case. The results strengthen the advantages of partial oxy-combustion in terms of significant decrease of the energy requirements in the solvent regeneration process and they might make partial oxy-combustion more feasible than post-combustion and oxy-combustion for CCS applications. Future investigation in this CCS technology will require the evaluation of the O_2-enriched air production should be investigate to evaluate the integration of the full partial oxy-combustion technology.

Acknowledgements

This work was carried out with the financial support of the Ministry of Economy and Competitiveness of the Spanish Government (OXYSOLVENT Pro.; ref: CTM-2014-58573-R) co-financed by the European Development Research Fund (EDRF) From European Union.

Special mention to José Antonio Camino Fernández for his esteemed contribution to this research work.

Annex

The CO_2 mass balance was calculated from the recorded data measured for each experiment. The aim of determining the CO_2 mass balance is to use it as a validation tool for the results summarized above. With regard to the mass balance of the entire lab-scale plant, the sum of the amounts of CO_2 measured at the stripper and absorber exhausts were within a 10% of deviation from the CO_2 introduced at the absorber inlet in all the runs.

A more accurate evaluation of the CO_2 mass balance was determined using the absorber as control volume. The total amount of CO_2 transferred from the gas phase to the liquid phase in the absorber was calculated in two different ways and the difference arising from the two

methods was subsequently compared. From the gas side, the calculation of the total CO_2 mass flow-rate transferred was based on the different CO_2 mass flow-rates between the gas inlet and outlet using the CO_2 concentration measurements and the mass-flow meters. From the liquid side, the calculations used the mean average cyclic capacity of the solvent calculated from the TOC measurements and the solvent flow-rate provided by the Coriolis flow meter. The comparison was plotted in Fig. 8.

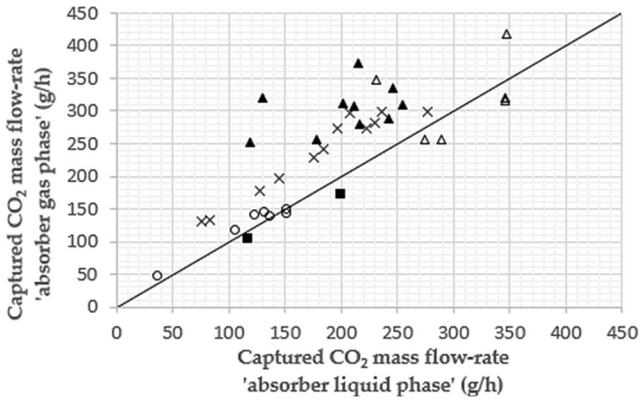

Figure 8. Comparison of the CO_2 mass flow-rate transferred from the gas phase to the liquid phase in the absorber: references (■), 20%v/v CO_2 experiments (○), 40%v/v CO_2 experiments (×) and 60%v/v CO_2 experiments using fresh (△) and used solvent (▲)

Most of the experiments showed higher transferred CO_2 mass flow-rates from the gas phase calculations. The CO_2 mass balance was within a deviation of 15% in those cases. The imbalance might be due to measurement errors and the use of average values. For example, small variations in the cyclic capacity may produce higher deviations in the calculation from the liquid side. A certain MEA degradation may also cause errors in the CO_2 mass balance calculations.

References

[1] International Energy Agency, Key World Energy Statistics 2017. IEA Report, 2017.

[2] M. Wang, A.S. Joel, C. Ramshaw, D. Eimer, N.M. Musa, Process intensification for post-combustion CO_2 capture with chemical absorption: A critical review, Appl. Energy 158 (2015) 275-291.

[3] D.P. Hanak, A.J. Kolios, V. Manovic, Comparison of probabilistic performance of calcium looping and chemical solvent scrubbing retrofits for CO_2 capture from coal-fired power plant, Appl. Energy 172 (2016) 323-336.

[4] UN Framework on Climate Change (UNFCCC). Adoption of the Paris agreement. Paris, France: United Nations Framework Convention on Climate Change, 2015.

[5] International Energy Agency, Carbon capture and storage: the solution for deep emissions reductions. Paris, France: IEA Publications, 2015.

[6] International Energy Agency, Energy technology perspectives 2015. Paris, France: IEA Publications, 2015.

[7] G.T. Rochelle, Thermal degradation of amines for CO_2 capture, Curr. Opin. Chem. Eng. 1 (2012) 183‑190.

[8] X. Chen, G. Huang, C. An, Y. Yao, S. Zhao, Emerging N-nitrosamines and N-nitramines from amine-based postcombustion CO_2 capture ‑ a review, Chem. Eng. J. 335 (2018) 921‑935.

[9] DOE-NETL, Cost and performance for low-rank pulverized coal oxy-combustion energy plants. Report n° 401/093010, 2010.

[10] E.O. Agbonghae, K.J. Hughes, D.B. Ingham, L. Ma, M. Pourkashanian, Optimal process design of commercial-scale amine-based CO_2 capture plants, Ind Eng Chem Res 53 (2014) 14815–14829.

[11] H.M. Kvamsdal, M.C. Romano, L. Van der Ham, D. Bonalumi, P. Van Os, E. Goetheer, Energetic evaluation of a power plant integrated with a piperazine-based CO_2 capture process, Int J Greenhouse Gas Control 28 (2014) 343–55.

[12] M.R.M. Abu-Zahra, J.P.M. Niederer, P.H.M. Feron, G.F. Versteeg, CO_2 capture from power plants: Part II. A parametric study of the economical performance based on mono-ethanolamine, Int J Greenhouse Gas Control 1 (2007) 135–142.

[13] H. Gao, B. Xu, H. Liu, Z. Liang, Effect of amine activators on aqueous N, N-diethylethanolamine solution for postcombustion CO_2 capture, Energy & Fuels 30 (2018) 7481-7488.

[14] Y. Shen,, C. Jiang, S. Zhang, J. Chen, L. Wang, J. Chen, Biphasic solvent for CO_2 capture: Amine property-performance and heat duty relationship, Appl Energy 230 (2018) 726-733.

[15] R. Santiago, J. Lemus, D. Moreno, C. Moya, M. Larriba, N. Alonso-Morales M.A. Gilarranz, J.J. Rodríguez, J. Palomar, From kinetics to equilibrium control in CO_2 capture columns using Encapsulated Ionic Liquids (ENILs), Chem Eng J 348 (2018) 661-668.

[16] D. Wang, S. Li, F. Liu, L. Gao, J. Sui, Post combustion CO_2 capture in power plant using low temperature steam upgraded by double absorption heat transformer, Appl Energy 227 (2018) 603-612.

[17] S.Y. Oh, S. Yun, J.K. Kim, Process integration and design for maximizing energy efficiency of a coal-fired power plant integrated with amine-based CO_2 capture process, Appl Energy 216 (2018) 311-322.

[18] Y.J. Lin, G.T. Rochelle, Approaching a reversible stripping process for CO_2 capture, Chem Eng J 283 (2016) 1033-1043.

[19] K. Goto, H. Okabe, F.A. Chowdhury, S. Shimizu, Y. Fujioka, M. Onoda, Development of novel absorbents for CO_2 capture from blast furnace gas, Int J Greenhouse Gas Control 5 (2011) 1214–1219.

[20] J. N. Knudsen, J.N. Jensen, P.J. Vilhelmsen, O. Biede, Experience with CO_2 capture from coal flue gas in pilot-scale: Testing of different amine solvents, Energy Proc 1 (2009) 783–790.

[21] E.S. Hamborg, V. Smith, T. Cents, N. Brigman, O.F. Pedersen, T. De Cazenove, M. Chhaganlal, et al., Results from MEA testing at the CO_2 technology centre Mongstad. Part II: Verification of baseline results, Energy Proc 63 (2014) 5994–6011.

[22] R. Notz, H.P. Mangalapally, H. Hasse, Postcombustion CO_2 capture by reactive absorption: Pilot plant description and results of systematic studies with MEA, Int J Greenhouse Gas Control 6 (2012) 84-112.

[23] H.P. Mangalapally, R. Notz, N. Asprion, G. Sieder, H. Garcia, H. Hasse, Pilot plant study of four new solvents for postcombustion carbon dioxide capture by reactive absorption and comparison to MEA, Int J Greenhouse Gas Control 8 (2012) 205–216.

[24] N.S. Kwak, J.H. Lee, I.Y. Lee, K.R. Jang, J.G. Shim, A study of the CO_2 capture pilot plant by amine absorption, Energy 47 (2012) 41–46.

[25] P. Moser, S. Schmidt, G. Sieder, H. Garcia, T. Stoffregen, Performance of MEA in a long-term test at the post-combustion capture pilot plant in Niederaussem, Int J Greenhouse Gas Control 5 (2011) 620–627.

[26] T. Hirata, H. Nagayasu, T. Yonekawa, M. Inui, T. Kamijo, Y. Kubota, T. Tsujiuchi, D. Shimada, T. Wall, J. Thomas, Current status of MHI CO_2 capture plant technology, 500 tpd CCS demonstration of test results and reliable technologies applied to coal fired flue gas, Energy Proc 63 (2014) 6120–6128.

[27] Z. Xu, S. Wang, J. Liu, C. Chen, Solvents with low critical solution temperature for CO_2 capture, Energy Proc 23 (2012) 64–71.

[28] S. Nakamura, Y. Yamanaka, T. Matsuyama, S. Okuno, H. Sato, Y. Iso, J. Huang, Effect of combinations of novel amine solvents, processes and packing at IHI's Aioi pilot plant, Energy Proc 63 (2014) 687–692.

[29] Ferrybridge power station. Carbon capture pilot project (CCPilot100+). <https://www.power-technology.com/projects/ferrybridge-ccpilot-100-power-station/>; 2018 [Access July, 2018].

[30] J.G. Thompson, S. Bhatnagar, M. Combs, K. Abad, F. Onneweer, J. Pelgen, D. Link, J. Figueroa, H. Nikolic, K. Liu, Pilot testing of a heat integrated 0.7MWe CO_2 capture system with two-stage air-stripping: Amine degradation and metal accumulation, Int J Greenhouse Gas Control 64 (2017) 23-33.

[31] M. Rabensteiner, G. Kinger, M. Koller, C. Hochenauer, Pilot plant study of aqueous solution of piperazine activated 2-amino-2-methyl-1-propanol for post combustion carbon dioxide capture, Int J Greenhouse Gas Control 51 (2016) 106-117.

[32] S., Karl, Start-up of world's first commercial post-combustion coal fired CCS project: Contribution of Shell Cansolv to SaskPower Boundary Dam ICCS project, Energy Proc 63 (2014) 6106–6110.

[33] E. Favre, R. Bounaceur, D. Roizard, A hybrid process combining oxygen enriched air combustion and membrane separation for post-combustion carbon dioxide capture, Sep. Purif. Technol. 68 (2009) 30‑36.

[34] A. Doukelis, I. Vorrias, P. Grammelis, E. Kakaras, M. Whitehouse, G. Riley, Partial O_2-fired coal power plant with post-combustion CO_2 capture: a retrofitting option for CO_2 capture ready plants, Fuel 88 (2009) 2428‑2436.

[35] F. Vega, M. Cano, S. Camino, B. Navarrete, J.A. Camino, Evaluation of the absorption performance of amine-based solvents for CO_2 capture based on partial oxy-combustion approach, Int. J. Greenhouse Gas Control 73 (2018) 95-103.

[36] F. Vega, A. Sanna, M.M. Maroto-Valer, B. Navarrete, D. Abad-Correa, Study of the MEA degradation in a CO_2 capture process based on partial oxy-combustion approach, Int. J. Greenhouse Gas Control 54 (2016) 160‑167.

[37] F. Vega, M. Cano, A. Sanna, J.M. Infantes, M.M. Maroto-Valer, B. Navarrete, Oxidative degradation of a novel AMP/AEP blend designed for CO_2 capture based on partial oxy-combustion technology, Chem Eng J 350 (2018) 883-892.

[38] G. Cau, V. Tola, F. Ferrara, A. Porcu, A. Pettinau, CO_2-free coal-fired power generation by partial oxy-fuel and postcombustion CO_2 capture: Techno-economic analysis, Fuel 214 (2018) 423-435.

[39] Y. Huang, M. Wang, P. Stephenson, S. Rezvani, D. Mcllveen-Wright, A. Minchener, N. Hewitt, A. Dave, A. Fleche, Hybrid coal-fired power plants with CO_2 capture: a technical and economic evaluation based on computational simulations, Fuel 101 (2012) 244‑253.

[40] C.C. Chen, L.B. Evans, A local composition model for the excess Gibbs energy of aqueous electrolyte solutions, AIChE J 32 (1986) 444-454.

[41] R.J. Little, G.F. Versteeg, W.P.M. Van Swaaij, Kinetics of CO_2 with primary and secondary amines in aqueous solutions – II. Influence of temperature on zwitterion formation and deprotonation rates, Chem Eng Sci 47 (1992) 2037-2045.

[42] C. Dinca, A. Badea, L. Stoica, A. Pascu, Absorber design for the improvement of the efficiency of postcombustion CO_2 capture, J Energy Inst 88 (2015) 304-313.

[43] P. Brúder, F. Owrang, H.F. Svendsen, Pilot study—CO_2 Capture into aqueous solutions of 3-methylaminopropylamine (MAPA) activated dimethyl-monoethanolamine (DMMEA). Int J Greenhouse Gas Control 11 (2012) 98-109.

[44] F.A. Tobiesen, O. juliussen, H.F. Svendsen, Experimental validation of a rigorous desorber model for CO_2 post-combustion capture, Chem Eng Sci 63 (2008) 2641-2656.

[45] R.E. Dugas, Pilot plant study of carbon dioxide capture by aqueous monoethanolamine, Thesis, University of Texas, 2006.